Available online at www.sciencedirect.com
ScienceDirect
Journal of the European Ceramic Society 29 (2009) 2211–2218
www.elsevier.com/locate/jeurceramsoc

Damage evaluation of two alumina refractory castables

M. Ghassemi Kakroudi [a], M. Huger [b,*], C. Gault [b], T. Chotard [b,*]

[a] *Department of Ceramic Engineering, University of Tabriz, Islamic Republic of Iran*
[b] *Groupe d'Etude des Matériaux Hétérogènes (GEMH), ENSCI, 47 Avenue Albert Thomas, 87065 Limoges Cedex, France*

Received 13 November 2008; received in revised form 15 December 2008; accepted 19 December 2008
Available online 16 April 2009

Abstract

The accumulation of damage by thermal treatment and its development under uniaxial loading–unloading cycles performed at room temperature has been evaluated for two alumina based refractory castables; an ultra low cement content bauxite material (Bau-ULCC) and a low cement content andalusite material (And-LCC).

Both castables exhibit notable damage with a level related to the firing temperature. The tensile behaviour is characterised by an elastic domain at the beginning of loading followed by a non-linear evolution up to the peak. In addition to the non-linearity of the stress–strain curve, the evolution of the loading–unloading cycle characteristics confirms the development of diffuse damage within the materials. In order to better understand the damage behaviour of the studied materials, the evolution of various parameters in relation with to the extent of damage has been analysed. These parameters are Young's modulus measured at the beginning of each unloading step E^i_{un}, the residual strain after each cycle ε^i_{res} and the associated consumed energy during the test (W^i_h).

The parameters extracted from the stress–strain curve reveal some interesting analogies between the two materials. In particular, it seems that a parameter D_{Th}, which quantifies the damage resulting from the thermal treatment, plays a major role in the mechanical behaviour until failure in a similar way for the two castables. It appears that the origin of damage in the two studied materials mechanically loaded after heat treatment is mainly thermal.

Keywords: Tensile test; Damage behaviour; C. Thermal expansion; E. Refractories; Castables

1. Introduction

The share of monolithic refractories in refractory application is growing worldwide. In general, fired refractory bricks can be advantageously replaced by monolithics, in terms of production cost, installation efficiency, safety and material consumption.[1] Refractory castables are subjected to severe loading, especially from a thermomechanical point of view and are degraded by a combination of several mechanisms including mainly thermal shock, mechanical impact, abrasion, and corrosion. The behaviour of these materials subjected to such mechanisms is influenced by many factors such as their chemical composition, their microstructure, as well as phase transformations, which occur at high temperature during firing process, and/or in service.[2]

In the metallurgical industry, refractory materials are used under high temperature conditions and are frequently subjected to thermal shocks. Consequently, these materials are damaged by thermal stress induced by temperature gradients. So far, few studies on this type of damage exist in the industry.[3,4]

Damage is not directly measurable. Many researches on damage evaluation have been reported based on various techniques such as optical or SEM observations of cracks, ultrasonic and acoustic methods[5–8] or mechanical testing[9–11] for measuring the different parameters which are sensitive to damage (ultrasonic velocity, attenuation coefficient), and especially the elastic moduli which appear to be typical and very good markers of damage evolution within the materials. The aim of this paper is to evaluate and to characterise the damage due to thermal and mechanical loading in these two alumina refractory castables thanks to uniaxial tensile tests performed after treatment at various temperature. From the results of loading–unloading cyclic tests, damage accumulation has been evaluated, and damage mechanisms have been proposed for the two materials.

* Corresponding authors.
E-mail addresses: marc.huger@unilim.fr (M. Huger), thierry.chotard@unilim.fr (T. Chotard).

0955-2219/$ – see front matter © 2009 Elsevier Ltd. All rights reserved.
doi:10.1016/j.jeurceramsoc.2008.12.019

Table 1
Chemical analysis and physical data for the two studied refractories.

Castable type	And-LCC	Bau-ULCC
Aggregate type	Andalusite	Bauxite
Al_2O_3 (wt%)	58	85
SiO_2 (wt%)	37.5	10
CaO (wt%)	2.3	1.1
Fe_2O_3 (wt%)	0.9	1
Max. aggregate size (mm)	5	5
Water requirement (wt%)	4.5–5.5	4.2–5.2
Open porosity (vol.%)	6	10
Apparent density (kg/m^3)	2600	2970

2. Materials and experimental procedures

2.1. Materials and samples preparation

Two commercial castables are considered. The first one is a low cement andalusite castable (And-LCC) made of andalusite aggregates, fumed silica, alumina and calcium aluminate cement. The second is an ultra low cement bauxite castable (Bau-ULCC) made of bauxite aggregates, fumed silica, alumina and the same cement. Both materials are characterised by the same fumed silica content. In Bau-ULCC, the alumina content is two times higher than in And-LCC. Table 1 shows the chemical compositions of the castables supplied by the manufacturer. The high difference between the silica contents of the two materials is mainly due to the high silica content in andalusite aggregates compared to bauxite ones. For both castables, the maximum aggregate size is about 5 mm. After reception from the manufacturer, the material raw samples (160 mm × 40 mm × 40 mm) were cured under air during 24 h at 110 °C. Fig. 1 shows pictures of polished sections of cured materials.

On this figure, one observes aggregates of sizes up to 5 mm, embedded in the matrix. The aggregates of large size will rather contribute to the mechanical reinforcement of the material whereas the finest particles, contained in the matrix, will play a significant role in the physicochemical reactions.

After machining, the final samples have been fired at 250, 500, 700, 900 and 1100 °C in order to simulate several thermal histories before characterisation. These temperature levels have been fixed according to the temperature range to which the refractory castables are subjected in specific industrial applications. Firing thermal cycles are characterised by 5 °C/min heating and cooling rates and by a 5 h isothermal dwell at the maximum firing temperature.

2.2. Tensile tests

Tensile tests have been performed with an INSTRON 8862 electro-mechanical universal testing machine at room temperature. Fig. 2 presents a schematic of the tensile test device. The strain is measured by two extensometers equipped by silicon carbide rods which are placed on two opposite sides of the specimen. The extensometer gauge length is 25 mm.

The low values of the displacement at rupture exhibited by refractories (3–5 μm) required a good control of the thermal stability of the extensometers (±0.1 °C). Samples are constituted of a cylindrical rod (18 mm in diameter) with two metallic parts glued at each end. The geometry is precisely adjusted thanks to a final cylindrical machining step of the total assembly. The tensile tests were carried up to rupture with a constant displacement velocity of 0.04 mm min^{-1}, with intermediate unloading at several level of stress. To accurately determine the Young's modulus, the "early" slope of the stress–strain curve has been determined. "Early" means here that the slope has been calculated in the very first loading step for a level of stress sufficiently low to insure that the linear part of the stress–strain curve is concerned.

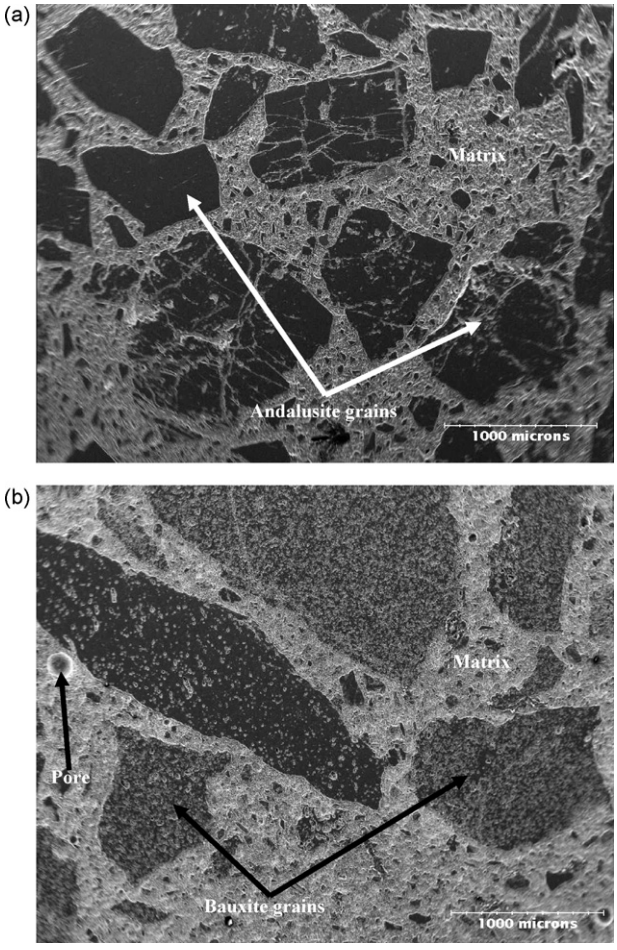

Fig. 1. Microstructure of the studied refractories: (a) And-LCC and (b) Bau-ULCC.

Fig. 3 illustrates a typical non-linear stress–strain behaviour issued from tensile test carried out on refractory castables. In order to perform a quantitative analysis of the damage process, different parameters have been extracted from the curves:

- E_0: initial Young's modulus corresponding to the first loading step.
- σ_{Peak}: maximum stress.
- ε_{Peak}: strain at maximum stress.
- σ_{Ult}: ultimate stress corresponding to the stress where final rupture occurs (similar to σ_{Peak} when there is not post-peak behaviour).

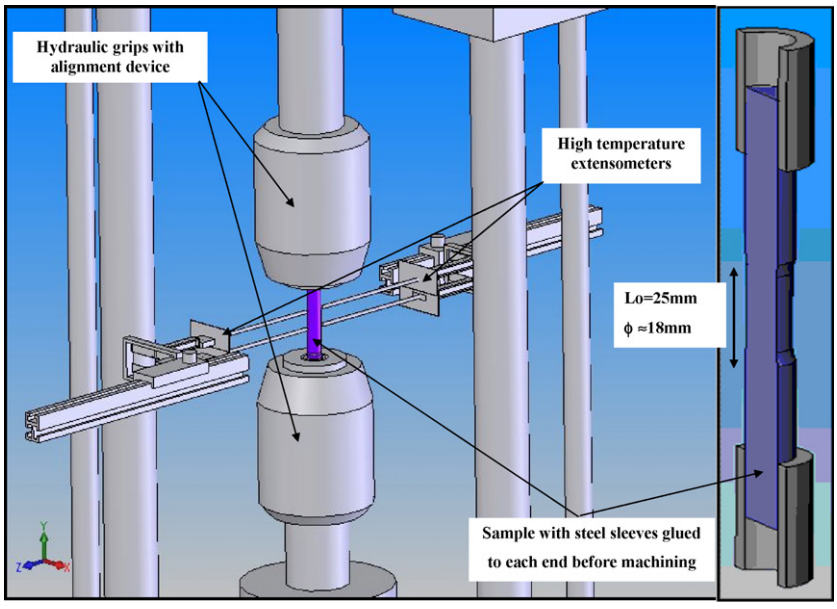

Fig. 2. Scheme of the tensile test device.

- ε_{Ult}: strain at σ_{Ult}.
- ε^i_{res}: residual strain at the end of ith cycle.
- E^i_{Un}: Young's modulus at the beginning of the unloading stage of the ith cycle.
- E^i_L: Young's modulus at the beginning of the loading stage of the $i+1$th cycle.
- W^i_h: energy dissipated within the material between the ith unloading cycle and $i+1$th loading cycle (hysteretic energy) per unit of volume.

3. Results and discussion

3.1. Mechanical behaviour in tension after thermal treatment

Previous measurements have highlighted that the elastic properties of the materials at room temperature are strongly dependent on their thermal history.[12] The interest of the tensile tests is to supplement these data by the determination of behaviour laws up to rupture and to show the non-linear character of the material when it is subjected to a high level of stress. Tests were carried out at room temperature on samples each previously treated at distinct temperature (110, 250, 500, 700, 900, 1100 °C). An example of the obtained stress–strain curves is presented in Fig. 4. At the beginning of loading, the two materials present an elastic linear behaviour. Beyond this domain, the two materials exhibit a non-linear behaviour. It is important to note that this non-linear domain is much more extended for And-LCC (Fig. 4a) than for Bau-ULCC (Fig. 4b). According to this remark, it appears that the Bau-ULCC refractory can be considered as "more brittle" than the And-LCC one.

In order to better understand this difference in behaviour, Fig. 5a and b presents the evolution of E_0 and ε_{Peak}, respectively,

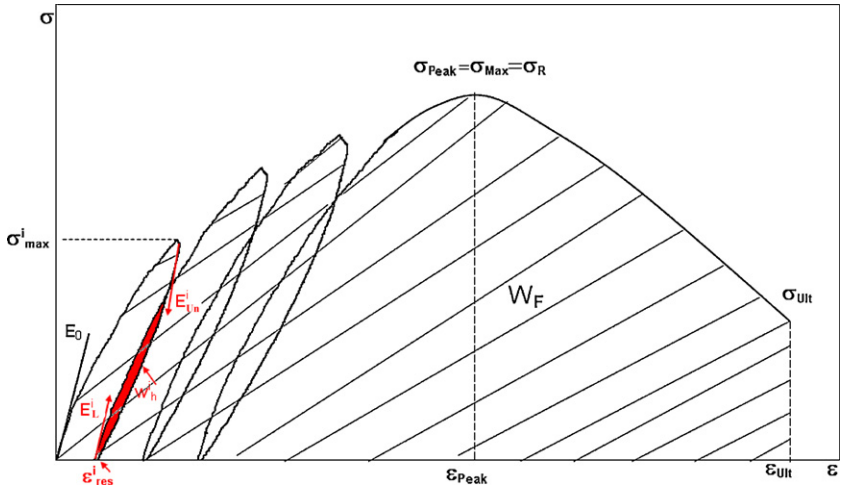

Fig. 3. Typical stress–strain curve in tension for refractory castables and its associated parameters.

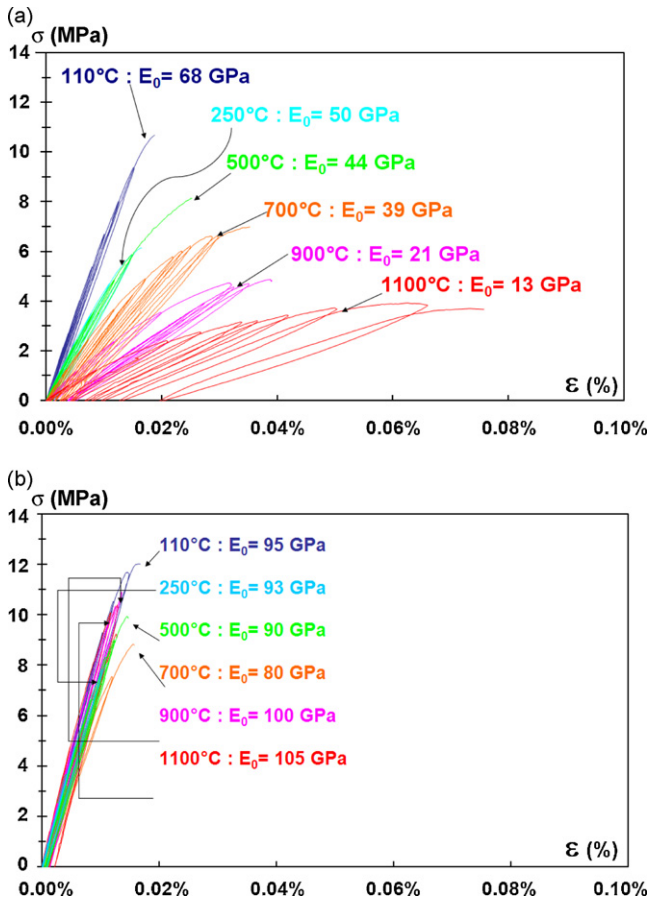

Fig. 4. Tensile behaviour at room temperature of both castables treated at different temperatures: (a) And-LCC and (b) Bau-ULCC.

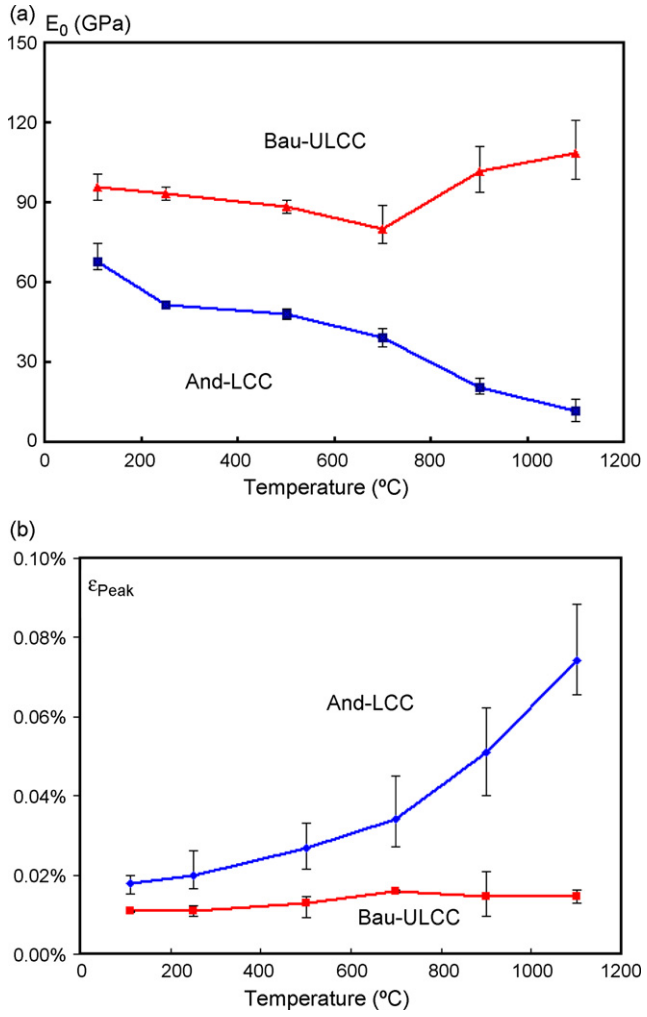

Fig. 5. Evolution of mechanical characteristics determined at room temperature for both castables vs. the temperature of treatment: (a) initial Young's modulus (E_0), (b) maximum strain (ε_{Peak}).

for the two castables according to the temperature of treatment. These results emphasise:

- a higher stiffness for Bau-ULCC than for And-LCC;
- a continuous reduction of the Young's modulus (E_0) after thermal treatments in the case of the And-LCC castable (Fig. 5a);
- a notable increase of ε_{Peak} (above 700 °C) in the case of the And-LCC castable (Fig. 5b);
- a increase of the Young's modulus (above 700 °C) after thermal treatments in the case of Bau-ULCC (Fig. 5a).

At the initial stage, after 110 °C, the And-LCC castable exhibits a rather linear elastic behaviour. Then, the behaviour moves from linear elastic to a non-linear one in the case of samples treated at higher temperature (Fig. 4a). The non-linear behaviour is magnified due to microcracking mechanisms which have been previously developed during the cooling stage of the thermal treatment. As temperature increases, E_0 decreases (Fig. 5a; from 68 GPa after a treatment at 110 °C to 13 GPa after a treatment at 1100 °C) while the maximum strain (ε_{Peak}, corresponding here to the strain-to-rupture) notably increases (Fig. 6; from 0.018 to 0.074%). This result shows that the damage, generated within this refractory by the initial heat treatment, most probably increases its capacity to exhibit a high level of strain before rupture.

In the case of Bau-ULCC castable, this evolution of tensile behaviour is very limited. After firing (up to 700 °C), the linear domain is reduced and a non-linear domain appears. As temperature increases, initial elastic property decreases (Fig. 5b; from 95 GPa after 110 °C to 80 GPa after 700 °C) while the maximum strain (ε_{Peak}) slightly increases but not in the same order of magnitude as for And-LCC (Fig. 6; from 0.012 to 0.016%). On the contrary, above 700 °C, E_0 increase (from 80 GPa at 700 °C to 105 GPa at 1100 °C). This increase of the Young's modulus associated to a slight decrease of ε_{Peak} (Fig. 5b) can be attributed to the presence of some impurities (e.g. TiO_2, Fe_2O_3, K_2O), within bauxite aggregates which induce the formation of vitreous phases promoting sintering processes at high temperature and the occurrence of viscosity in the mechanical behaviour of the material.

3.2. Damage analysis

A previous study[13] has revealed that, during heating, the two castables behave different, because of strong differences between matrix and aggregate behaviours. The results of tensile

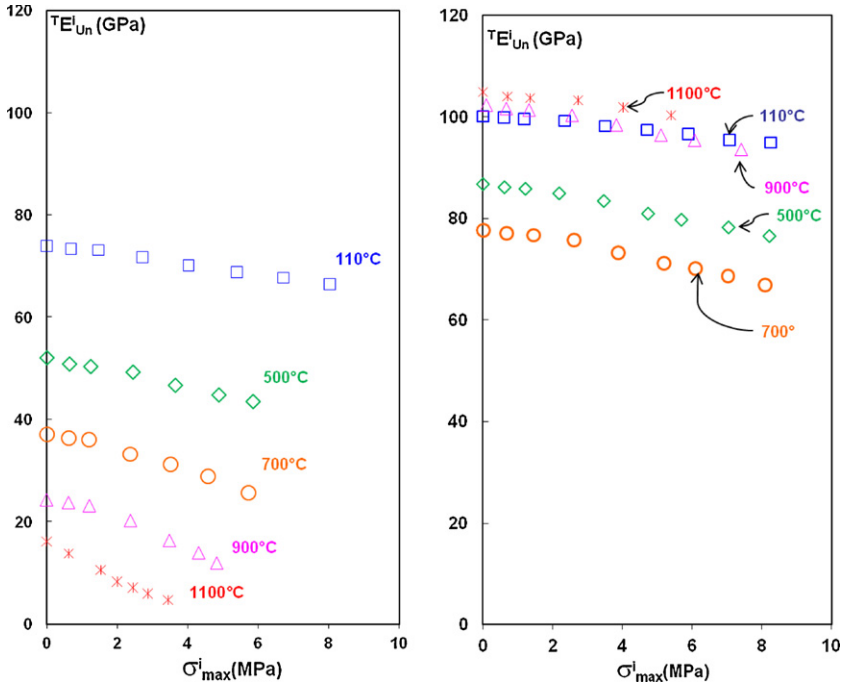

Fig. 6. Evolution of the modulus of elasticity measured at the beginning of the unloading stage (${}^{T}E^{i}_{\mathrm{Un}}$) vs. maximum stress reached at each cycle ($\sigma^{i}_{\max}$), for both castables previously treated at different temperatures: (a) And-LCC and (b) Bau-ULCC.

tests show an increase of the strain-to-rupture after heat treatment, because of the development of a diffuse damage, which adds to the network of decoherences and microscopic cracks already present in the material before the mechanical test. In addition to the non-linearity of the stress–strain curve, evolutions of the characteristics of the loading–unloading cycles confirm the development of such a diffuse damage, at the same time, by the decrease of the values of the modulus of elasticity at the beginning of the unloading stage (E^{i}_{Un}), by the evolution of the hysteretic loops in each cycle and also by the progressive increase in the area of these loops.

In order to better understand the damage behaviour of the studied materials, we have analysed and presented the evolution of various parameters in relation to their damage characters. These parameters are: the modulus of elasticity at the beginning of the unloading stage E^{i}_{Un}, the residual strain $\varepsilon^{i}_{\mathrm{res}}$ and the hysteretic energy W^{i}_{h}

3.2.1. Evolution of the modulus of elasticity at the beginning of the unloading stage E^{i}_{Un}

In order to compare the damage at the end of each maximum subjected stress $\sigma^{i}_{\max}$, Fig. 6 presents the evolution of E^{i}_{Un} for both studied castables.

It is important to note that the values plotted right on the y-axis correspond to initial moduli (taken at the beginning of loading) measured at room temperature and after preliminary heat treatment at different temperatures (noted thereafter ${}^{T}E_0$). At the end of each loading, the material stiffness evolves and then, the modulus of elasticity moves to take a new value quantified at the beginning of unloading step (${}^{T}E^{i}_{\mathrm{Un}}$), where T characterises the preliminary temperature of treatment and i the number of the considered mechanical loading cycle.

It is for the lowest temperature treatment (110 °C) that one observes, for the two castables, the smallest reduction in ${}^{T}E^{i}_{\mathrm{Un}}$ during loading/unloading cycles. The strongest evolution of this parameter is observed for And-LCC pre-treated at 1100 °C (Fig. 6a).

The evolution of ${}^{T}E^{i}_{\mathrm{Un}}$ during the mechanical cycles seems here to be related to the decrease of the ${}^{T}E_0$ values resulting from the thermal pre-treatment.

By regarding the value of ${}^{110}E_0$ as a reference value, the whole of the values presented in Fig. 6 make it possible to calculate several damage parameters on the basis of a Kachanov's type formula.

A damage parameter relating to the thermal treatment can be defined by the following equation:

$$D_{\mathrm{Th}} = \frac{(1 - {}^{T}E_0)}{{}^{110}E_0} \tag{1}$$

At the end of the thermal treatment, the mechanical loading generates an additional damage which results in defining a damage cumulated parameter $D_{\mathrm{Th+M}}$:

$$D_{\mathrm{Th+M}} = \frac{(1 - {}^{T}E^{I}_{\mathrm{Un}})}{{}^{110}E_0} \tag{2}$$

To facilitate the analysis of our results, these values have been calculated at a common stress level (equal to 4 MPa) for all tests. The choice of this level has been made by considering the higher common stress which has been found for all tensile tests and also for the two castables. Fig. 7 presents the evolution of the damage cumulated parameter $D_{\mathrm{Th+M}}$ (damage of thermal and mechanical origin) for the two materials, as a function of D_{Th} (only thermal origin damage). Despite the difference of the aggregates, the corresponding points for the two materials follow

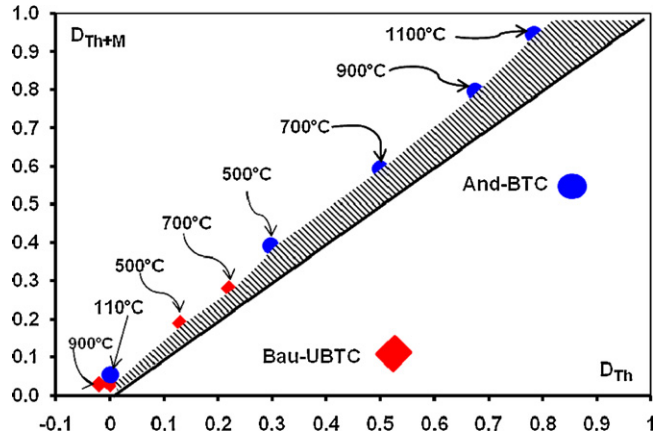

Fig. 7. Evolution of the parameter D_{Th+M} (superimposed damage from thermal and mechanical origin) according to D_{Th} (damage only from thermal origin) for both castables previously treated at different temperatures.

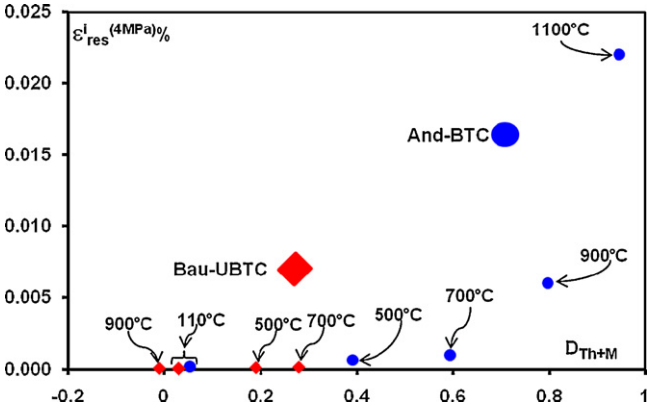

Fig. 9. Evolution of the residual strain ($\varepsilon_{res}^{i\,(4\,MPa)}$) according to the damage cumulated parameter D_{Th+M} for both castables previously treated at different temperatures.

the same tendency. The shaded zone reveals the contribution of the mechanical damage to the total damage. Globally, the contribution of the mechanical damage increases according to the level of thermal origin damage. In other words, the damage of the studied castables loaded mechanically after heat treatment is mainly prompted by damage from thermal origin.

In the case of the andalusite based castable (And-LCC), the values of the damage parameters increase with the preliminary thermal treatment. Until 700 °C, the same trend is observed for the bauxite base castable (Bau-ULCC). Beyond this temperature, a reversion of this tendency is noted most probably due to sintering phenomena.

3.2.2. *Evolution of the residual strain* ε_{res}^{i}

The study of the ${}^{T}E_{Un}^{i}$ evolution made it possible to highlight the development of damage during loading–unloading cycles. The cracks created during the loading time can generate a residual strain at the end of the unloading step because of their no closing state.

This no closing state can result from different mechanisms. On the one hand, the presence of debris opposes the re-contact of the free surfaces of the cracks and, on the other hand, the internal stress relaxation from the thermal expansion mismatch between phases in the vicinity of the cracks.

Fig. 8 illustrates the evolution of the residual strain (ε_{res}^{i} according to σ_{max}^{i}) for the two castables after thermal treatment at various temperatures. Generally, these results show that the residual strain ε_{res}^{i} is much more important in the case of the andalusite based castable (And-LCC).

The values of the residual strain, probably correlated with cracking within materials, Fig. 9 presents the variations of $\varepsilon_{res}^{i\,(4\,MPa)}$ according to the cumulated damage parameter D_{Th+M}.

As already observed in Fig. 7, the corresponding points for the two materials fit in the same curve. However, in the case

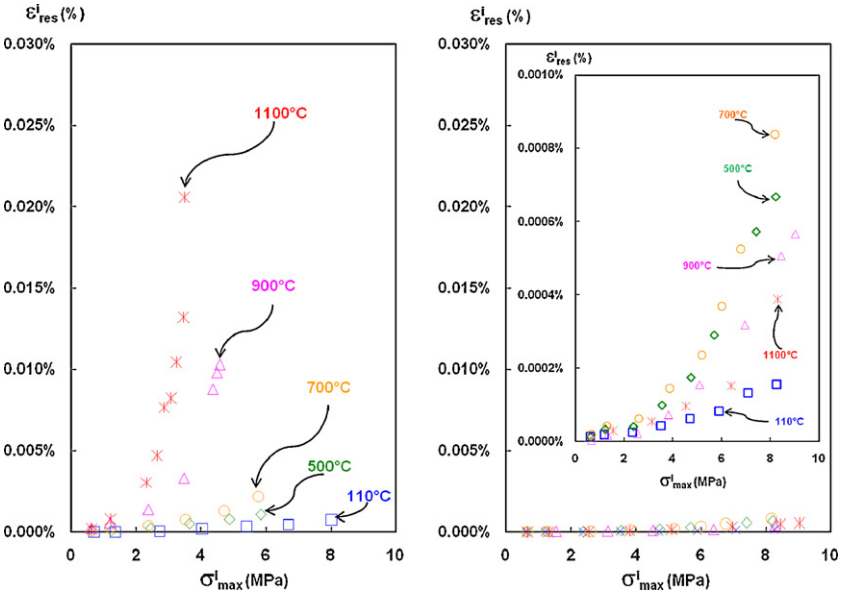

Fig. 8. Evolution of the residual strain (ε_{res}^{i}) according to the maximum stress for each cycle (σ_{max}^{i}) for both castables previously treated at different temperatures: (a) And-LCC, (b) Bau-ULCC with magnification.

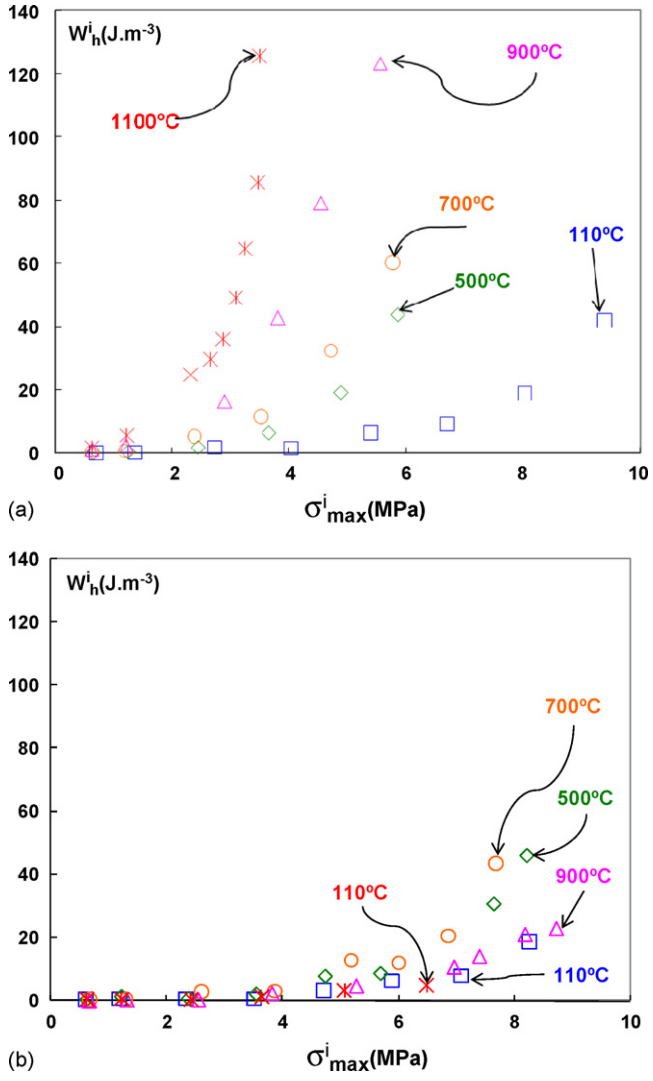

Fig. 10. Evolution of the hysteretic energy (W^i_h) per unit of volume according to the maximum stress of each cycle (σ^i_{max}) for both castables previously treated at different temperatures: (a) And-LCC and (b) Bau-ULC.

of the And-LCC castable treated at high temperatures (900 and 1100 °C), $\varepsilon^{i\,(4\,MPa)}_{res}$ increases in a significant way.

The high level of damage, potentially acceptable by this concrete treated at high temperature, probably leads to large openings of cracks during the mechanical loading thus facilitating the fall of debris which then, opposes their closing during mechanical unloading, and thus induce a higher level of residual strain.

3.2.3. *Evolution of the "hysteretic energy"* (W^i_h)

As seen in Fig. 4, the loading–unloading cycles presented on stress–strain curves of the two castables underline an hysteretic phenomenon most probably related to a dissipative energy process. In order to quantify for each cycle this energy process, W^i_h (in J m^{-3}) has been defined as the energy dissipated within the material between the ith unloading cycle and $i+1$th loading cycle and normalised by the value of the volume of the useful area of the test sample. Fig. 10 presents the evolution of W^i_h as a function of σ^i_{max} for the two castables treated at various temperatures.

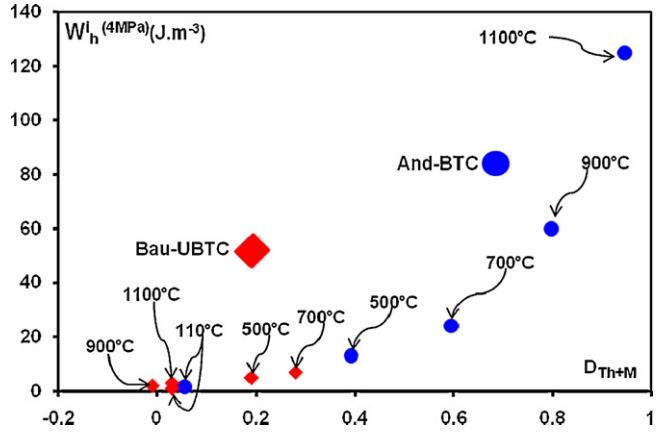

Fig. 11. Evolution of the hysteretic energy ($W^{i\,(4\,MPa)}_h$) according to the cumulated damage parameter D_{Th+M} for both castables previously treated at different temperatures.

In Fig. 10a, one can easily observes that the W^i_h values are notably higher in the case of the And-LCC castable. As the level of dissipated energy during loading–unloading cycles is most probably related to the surface of microscopic cracks present in materials, W^i_h has been represented in Fig. 11 according to the cumulated damage parameter D_{Th+M} and that for a maximum stress level equal to 4 MPa.

One more time, the corresponding points for the two materials follow the same trend. A very strong correlation is thus underlined between the energy dissipated during loading–unloading cycles and the damage level present in material. This energy dissipation is probably closely related to friction mechanisms which occur between the free surfaces of cracks. It is thus logical that W^i_h is directly related to the surface area of defects found in the material.

4. Conclusion

Both castables exhibit notable damage behaviours with a damage level related to the firing temperature. The tensile behaviour is characterised by a linear elastic domain at the beginning of loading followed by a non-linear evolution up to the peak. For a similar temperature, the extent of the non-linear domain for the And-LCC castable is higher than for the Bau-ULCC one because of damage development. In the case of the And-LCC, temperature cycling reduces the maximum strength, but strongly increases the compliance and the strain-to-rupture.

An original analysis, based on parameters extracted from tensile curves (E^i_{un}, ε^i_{res} and W^i_h) has underlined some interesting analogies between the two materials. In particular, it seems that the parameter D_{Th} (quantifying the damage resulting from the preliminary heat treatment) controls the mechanical behaviour up to rupture in a similar way for the two castables. It appears also that the damage of the two studied castables loaded mechanically after heat treatment is mainly from thermal origin.

Acknowledgements

The authors are grateful to the French Ministry of Economy and Industry for its financial support. Authors would

like to thank TRB Refractories Company for supplying the studied castables. One author, Dr Ghassemi-Kakroudi, is particularly thankful to the Iranian Ministry of Science and Technology and to the University of Tabriz for financial support.

References

1. Ningsheng, Z., Advances in modern refractory castables. In *Proc. of the First International Conference on Refractories*, 2004, pp. 148–154.
2. Serry, M. A. and Telle, R., Thermomechanical properties of high alumina castables. *Am. Ceram. Bull.*, 2000, **79**(11), 71–75.
3. Schmitt, N., Burr, A., Berthaud, Y. and Poirier, J., Micromechanics applied to the thermal shock behaviour of refractory ceramics. *Mech. Mater.*, 2002, **34**, 725–747.
4. Lee, W. J. and Case, E. D., Cyclic thermal shock in silicon carbide-whisker-reinforced alumina composite. *J. Mater. Sci.*, 1989, 113–119.
5. Huger, M., Fargeot, D. and Gault, C., High-temperature measurement of ultrasonic wave velocity in refractory materials. *High Temp.-High Press.*, 2002, **34**, 193–201.
6. Huger, M., Tessier-Doyen, N., Chotard, T. and Gault, C., Microstructural effects associated to CTE mismatch for enhancing the thermal shock resistance of refractories: investigation by high temperature ultrasounds. *Ceram. Forum Int.*, 2007, **9**, E93–E102.
7. Chotard, T., Soro, J., Lemercier, H., Huger, M. and Gault, C., High temperature characterisation of Cordierite-Mullite refractory by ultrasonic means. *J. Eur. Ceram. Soc.*, 2008, **28**, 2129–2135.
8. Briche, G., Tessier-Doyen, N., Huger, M. and Chotard, T., Investigation of damage behaviour of refractory model materials at high temperature by combined pulse echography and acoustic emission techniques. *J. Eur. Ceram. Soc.*, 2008, **28**, 2835–2843.
9. Jonas, J. J. and Baudelet, B., Effect of crack and cavity generation on tensile stability. *Acta Metal.*, 1977, **25**(1), 43–50.
10. Nazaret, F., Marzagui, H. and Cutard, T., Influence of the mechanical behaviour specificities of damaged refractory castables on the Young's modulus determination. *J. Eur. Ceram. Soc.*, 2006, **26**, 1429–1438.
11. Bradt, R. C., Elastic moduli, strength and fracture characteristics of refractories. *Key Eng. Mater.*, 1993, **88**, 165–191.
12. Ghassemi kakroudi, M., Yeugo-Fogaing, E., Huger, M., Chotard, T. and Gault, C., Thermal history and mechanical properties of alumina castables. In *10th European Ceramic Congress*, 2007.
13. Ghassemi kakroudi, M., Yeugo-Fogaing, E., Huger, M., Chotard, T. and Gault, C., Effect of thermal treatment on damage mechanical behaviour of refractory castables: comparison between bauxite and andalusite aggregates. *J. Eur. Ceram. Soc.*, 2008, **28**, 2471–2478.